Please cite this article in press as: Peterson and Krasnow, Subcellular Trafficking of FGF Controls Tracheal Invasion of *Drosophila* Flight Muscle, Cell (2015), http://dx.doi.org/10.1016/j.cell.2014.11.043

Article

Cell

Subcellular Trafficking of FGF Controls Tracheal Invasion of *Drosophila* Flight Muscle

Soren J. Peterson[1] and Mark A. Krasnow[1,*]
[1]Howard Hughes Medical Institute and Department of Biochemistry, Stanford University School of Medicine, Stanford, CA 94305-5307, USA
*Correspondence: krasnow@stanford.edu
http://dx.doi.org/10.1016/j.cell.2014.11.043

SUMMARY

To meet the extreme oxygen demand of insect flight muscle, tracheal (respiratory) tubes ramify not only on its surface, as in other tissues, but also within T-tubules and ultimately surrounding every mitochondrion. Although this remarkable physiological specialization has long been recognized, its cellular and molecular basis is unknown. Here, we show that *Drosophila* tracheoles invade flight muscle T-tubules through transient surface openings. Like other tracheal branching events, invasion requires the Branchless FGF pathway. However, localization of the FGF chemoattractant changes from all muscle membranes to T-tubules as invasion begins. Core regulators of epithelial basolateral membrane identity localize to T-tubules, and knockdown of AP-1γ, required for basolateral trafficking, redirects FGF from T-tubules to surface, increasing tracheal surface ramification and preventing invasion. We propose that tracheal invasion is controlled by an AP-1-dependent switch in FGF trafficking. Thus, subcellular targeting of a chemoattractant can direct outgrowth to specific domains, including inside the cell.

INTRODUCTION

Insect flight is powered by flight muscles that have the highest known rates of cellular metabolism (Weis-Fogh, 1961, 1964). The oxygen used in aerobic respiration during flight is delivered by an extensive network of air-filled tracheae that ramify not only on the surface of the flight muscle, as in other tissues, but also within muscle plasma membrane invaginations that extend deep inside the myocytes. These fine tracheal branches encircle every mitochondrion of the flight muscle, delivering oxygen directly to where it is used (Smith, 1961a; Weis-Fogh, 1964; Wigglesworth and Lee, 1982; Meyer, 1989). The presence of tracheae within insect flight muscle was first noted over a century ago by Leydig and Ramon y Cajal in the initial descriptions of muscle substructure (Leydig, 1859; Cajal, 1890) and was later elaborated by early electron microscopy (EM) studies (Smith, 1961b). However, the developmental, cellular, and molecular basis of this remarkable structural specialization to accommodate the extreme physiology of flight muscle is unknown.

The Branchless FGF signaling pathway controls tracheal branching throughout development of the fruit fly *Drosophila melanogaster*. In the embryo, tracheal progenitor cells begin to express *breathless* (*btl*) FGF receptor (Glazer and Shilo 1991), while *branchless* (*bnl*) FGF gene turns on in a complex and dynamic pattern in small clusters of cells surrounding the progenitors (Sutherland et al., 1996). Bnl FGF functions as a chemoattractant, activating Btl FGFR and directing branch budding and outgrowth of the stereotyped primary and secondary tracheal branches. *bnl* turns on again later during larval development, its expression now controlled by the oxygen needs of the target tissues (Jarecki et al., 1999). Oxygen starvation induces *bnl* expression, and the secreted FGF induces outgrowth of fine cytoplasmic processes from the tracheal terminal cells toward the hypoxic cell, ultimately forming fine terminal branches (tracheoles) that deliver oxygen to the cell. In this way, the tracheal system provides oxygen directly to most cells of the larva. During metamorphosis, dedifferentiated larval tracheal cells and imaginal tracheal progenitors that remain quiescent during early tracheal development become activated, and here too *bnl* is expressed at specific sites and directs the proliferation and outgrowth of tracheal cells to form pupal and adult branches (Weaver and Krasnow, 2008; Chen and Krasnow 2014) and the adult air sacs that fill much of the adult fly (Sato and Kornberg, 2002).

Here, we describe the development of tracheal branches that supply the indirect flight muscle of *Drosophila*, one of the adult muscles that powers flight. The muscle forms during pupal development and, as we describe below, receives its tracheal supply from progenitors that extend out to the developing flight muscle from a thoracic air sac. However, unlike other tracheal terminal branches, which ramify on the surface of their target cells, we show that flight muscle terminal branches "invade" the T-tubules, plasma membrane invaginations that extend deep within the myocyte interior to facilitate excitation-contraction coupling. We show that the Bnl FGF pathway directs not only tracheal outgrowth to the flight muscle as in other tissues, but also T-tubule invasion, and that invasion is activated by a developmental switch in Bnl trafficking that targets Bnl selectively to T-tubules.

RESULTS

Tracheae Invade Flight Muscle T-Tubules through Transient Surface Openings

Anatomical and ultrastructural studies (Leydig, 1859; Cajal, 1890; Smith, 1961a; Weis-Fogh, 1964) of indirect flight muscle

Please cite this article in press as: Peterson and Krasnow, Subcellular Trafficking of FGF Controls Tracheal Invasion of *Drosophila* Flight Muscle, Cell (2015), http://dx.doi.org/10.1016/j.cell.2014.11.043

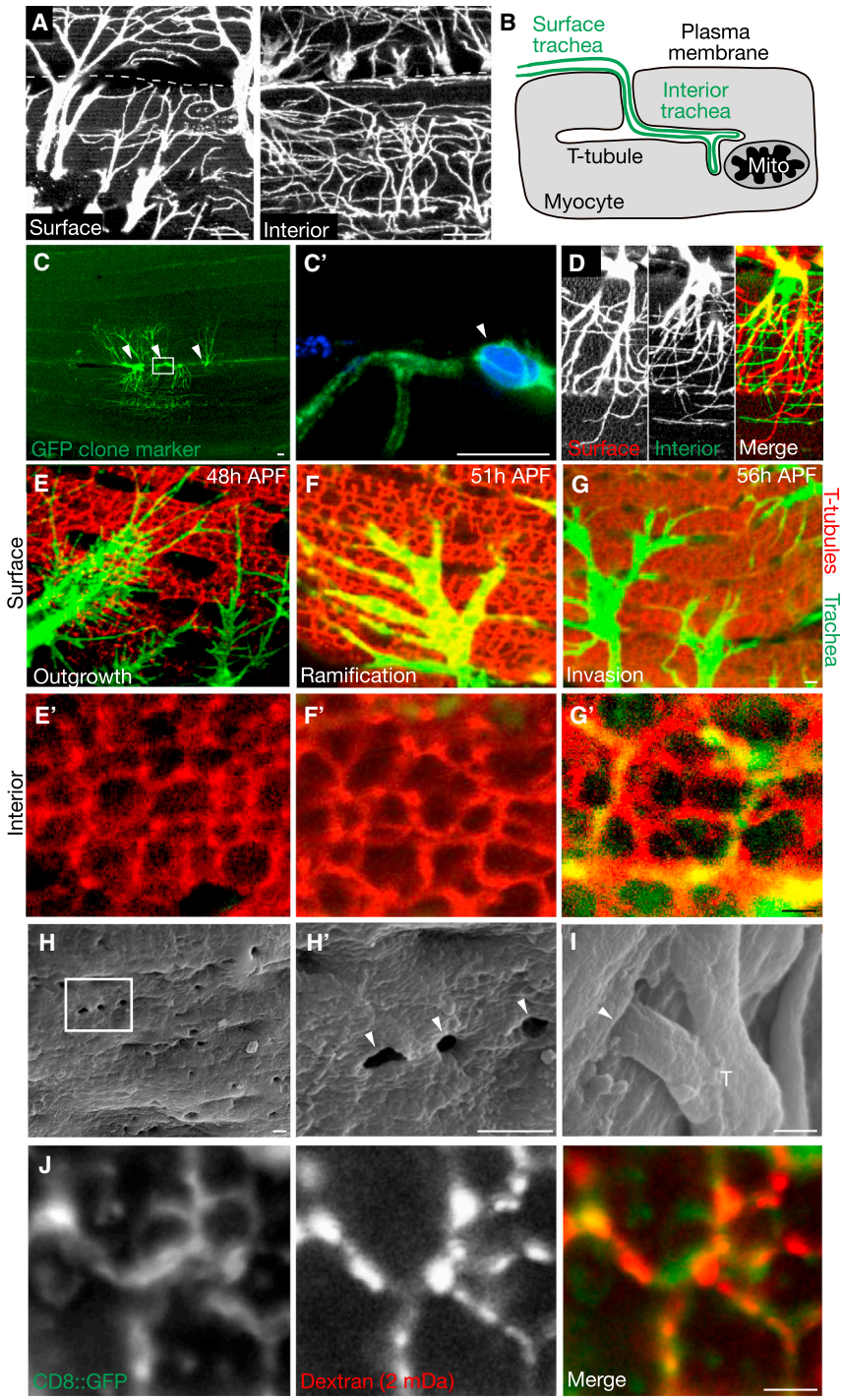

Figure 1. Tracheal Invasion of Flight Muscle T-Tubules

(A) Indirect flight muscle (dorsal longitudinal muscle, DLM) fiber of a *btl-Gal4*; *UAS-CD8-GFP* adult *Drosophila* showing tracheal branches (CD8-GFP immunostain, white) ramifying on muscle fiber surface (left) or interiorly 5 μm below the surface (right). Dashes, muscle fiber boundary.

(B) Schematic of tracheal branch (green) on surface of flight muscle fiber (Myocyte, gray) and continuing into T-tubule plasma membrane invagination to form internal trachea that terminate at mitochondria (Mito).

(C) Three terminal cells of a GFP-marked tracheal clone (green) generated by MARCM. Nuclei were stained with DAPI (blue); nuclei of the three terminal cells in the clone are indicated (arrowheads); boxed area (C′) shows soma of one of the marked cells. Somas of the three terminal cells lie between two fibers and each extends branches onto the surface of and within both neighboring fibers.

(D) Depth-coded confocal stack of single-cell tracheal MARCM clone. Tracheal branches on the muscle surface (red) narrow as they progress within the muscle fiber and become internal branches (green).

(E–G) Time course of tracheal outgrowth to flight muscle and T-tubule invasion. Flight muscle fibers of *btl-Gal4*; *UAS-CD8-GFP* pupae at the indicated times after puparium formation (APF) immunostained for trachea (GFP, green) and for T-tubules (amphiphysin, red). Upper panels (E–G), muscle fiber surface; lower panels (E′–G′), interior view of same fiber 5 μm below surface. Note tracheae ramifying on fiber surface in (E–G) but invasion of T-tubules only in (G′).

(H and I) Scanning electron micrographs of flight muscles 55 hr APF. T-tubule openings (~300 nm diameter) are visible at surface of fiber (H′, close up of boxed region in H). Trachea (T) enter some of the openings (I).

(J) Close-up of T-tubules (green) of *mef2-Gal4*; *UAS-CD8::GFP* 55 hr APF flight muscles incubated with 2 mDa fluorescent dextran for 20 min (red). Dextran has entered T-tubules (CD8::GFP, green), indicating that they are open to exterior. Scale bars represent 10 μm (A–D) and 1 μm (E–J).

See also Figure S1.

of *Drosophila* and other insects identified a dense array of tracheal branches (tracheoles) on the muscle surface (plasma membrane or sarcolemma) and within the T-tubule network deep below the surface (Wigglesworth and Lee, 1982) (Figures 1A and 1B). Analysis of *Drosophila* tracheal cell clones marked with CD8::GFP showed that individual tracheal cells formed multiple branches present on both the surface and interior of dorsal longitudinal flight muscle fibers (Figures 1C and 1D). To explore how and when this specialized tracheal network forms and reaches the muscle interior, we analyzed flight muscle tracheal development in transgenic *Drosophila* carrying btl-Gal4 > CD8::GFP to label tracheal cells and their cytoplasmic extensions and anti-Amphiphysin immunostaining (Razzaq et al., 2001) to label the T-tubule network. We focused our analysis on the dorsal longitudinal muscles (DLM) that are anchored to the thoracic cuticle by tendon cells and, along with the dorsal ventral muscles, are the two sets of nearly perpendicular muscles that comprise the indirect flight muscle (Figure S2A).

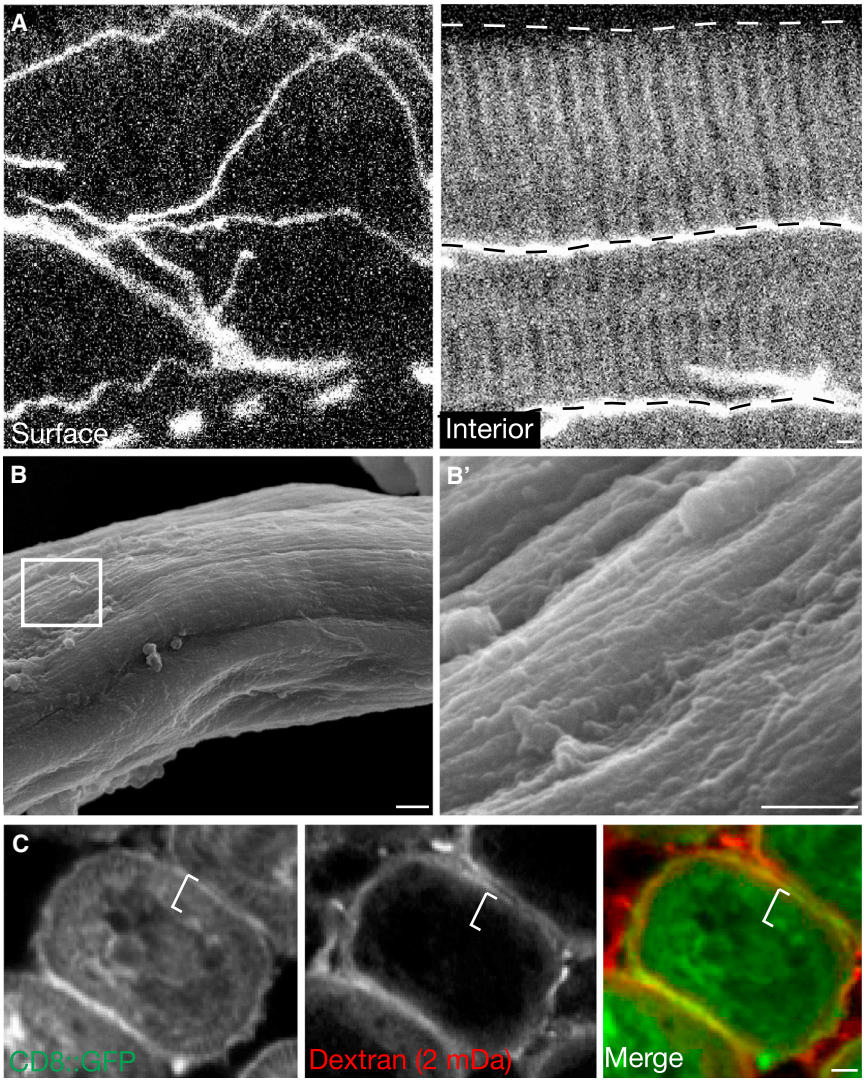

Figure 2. Muscles Not Invaded by Trachea Lack Surface Openings

(A) Surface (left) and interior (right) views of a plural remoter of coxae muscle fiber immunostained for D3 tracheal antigen (white) to show tracheal distribution. Trachea are present on surface and between fibers (dashed lines) but not inside individual fibers.

(B) Scanning electron micrograph of a 68 hr APF leg tubular muscle fiber during tracheal outgrowth. (B′) Detail of boxed region in (B). No T-tubule membrane openings are apparent on fiber surface.

(C) Cross section of adult leg tubular muscle of *mef2-Gal4*; *UAS-CD8::GFP* pupa 65 hr APF, after incubation with 2 mDa fluorescent dextran (red) for 20 min. Muscle membranes are marked with CD8::GFP (green). Dextran is detected on fiber surface but not in T-tubule region within fiber (white bracket). Scale bars represent 1 μm.

See also Figure S2.

The DLM begin to form at the onset of metamorphosis when a pool of myoblasts from the wing imaginal disc migrate to and fuse with specific "founder" larval myocytes, forming the nascent DLM muscle fibers by 24 hr after puparium formation (APF) (Dutta et al., 2004). The T-tubule network was present at 48 hr APF, when the medioscutal, lateroscutal, and scutellar air sacs extended tracheal projections that reached the muscle fibers (Figure 1E). Over the next 6–8 hr, the tracheal projections ramified and formed extensive networks of fine branches on the surface and between flight muscle fibers, but were not detected in the muscle interior (Figures 1F and 1F′). At ~55 hr APF, fine tracheal branches began to invade the T-tubule network (Figure 1G′). They entered T-tubules through ~300 nm surface openings that were visualized by scanning electron microscopy (Figures 1H and 1I) and accessible to 2 mDa (~50 nm diameter) (Dreher et al., 2006) dextran (Figure 1J). Tracheae invaded only some of the openings and then extended and ramified within the T-tubule network, ultimately filling just a small portion of the network (Figure 1G′). By 70 hr APF, invasion appeared complete, and the invaded T-tubules turned off the T-tubule marker amphiphysin while the other T-tubules maintained its expression (Figure S1A available online). Later, all flight muscle T-tubules constricted (Figures S1B and S1C) and surface accessibility was lost (Figure S1D). Thus, tracheal branches invade the flight muscle T-tubule network through large but transient surface openings during a 10–15 hr period of pupal development.

Muscles Not Invaded by Tracheae Lack Surface Openings

The tracheation pattern of other larval and adult thoracic and abdominal muscles was surveyed, and although all showed tracheal branching on their surface, none contained tracheae in their T-tubule networks in internal membrane networks (Figure 2A). When we examined one of them, the plural remoter of coxa tubular muscle (Figure S2A), by scanning electron microscopy (SEM) during the time its tracheae develop (Figure S2B), no openings in the muscle surface were detected (Figure 2B). Also, T-tubules of the leg muscle were not accessible to large dextrans (2 mDa or 500 kDa) that readily entered the T-tubular network of the indirect flight muscle (Figures 2C and S2C). Thus, other muscles lack the large surface openings through which trachea invade the indirect flight muscle T-tubule network.

The Branchless FGF Pathway Is Required for Flight Muscle Invasion

Bnl FGF directs tracheal outgrowth during development by activating the Btl FGFR expressed on tracheal cells. To determine if the Bnl pathway is required for flight muscle invasion, we examined the effect of *bnl* and *btl* mutations on the number of tracheal branches and branch points within individual flight muscle fibers. Because null mutations in either gene cause early lethality, we

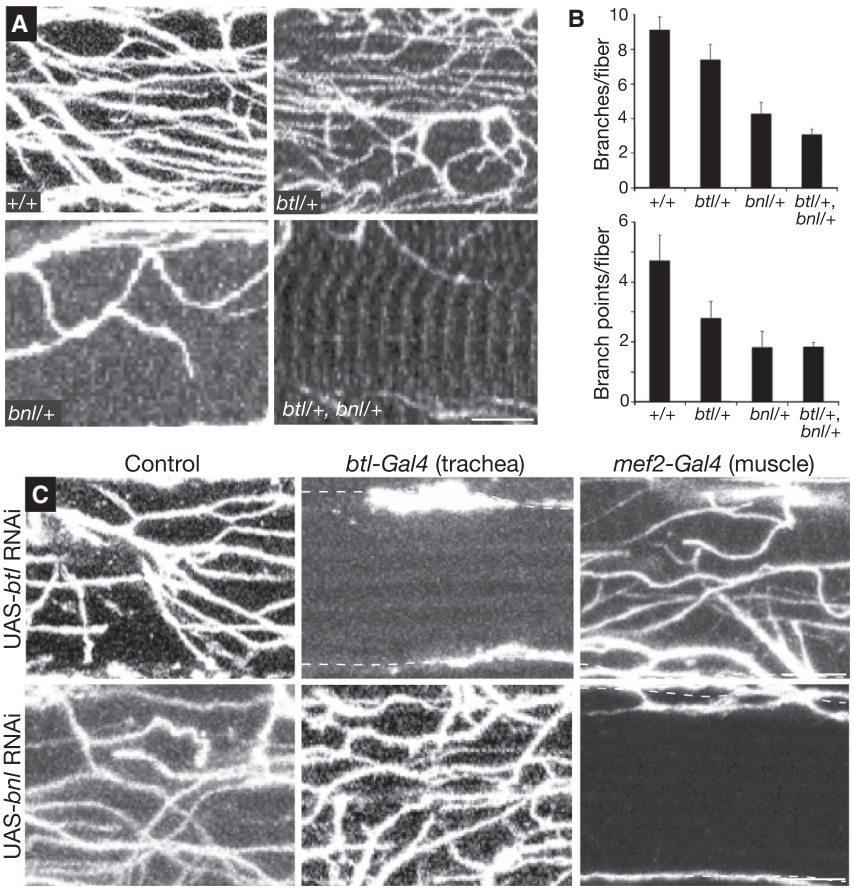

Figure 3. Effect of *breathless* FGFR and *branchless* FGF Mutations on Tracheal Invasion

(A) Interior views of single adult indirect flight muscle fibers of Oregon-R wild-type adult control (+/+) and adults of the indicated genotypes, immunostained for D3 antigen to show invaded trachea. *btl*, btl^{LG18} (null allele); *bnl*, bnl^{P1} (null allele).

(B) Quantification of tracheal branches and branch points per muscle fiber in genotypes as in (A) (n = 25 fibers scored for each genotype). Error bars represent SEM.

(C) Tissue-specific knockdown of *btl* and *bnl* using Gal4-UAS system. Interior view of single muscle fibers as above from adult controls (no Gal4 driver) or adults with knockdown of *btl* FGFR (UAS-btl [RNAi]) or *bnl* FGF (UAS-bnl [RNAi]) in the tracheal system (*btl-Gal4* driver) or flight muscle (*mef2-Gal4* driver), as indicated. All animals contained a *tubulin-Gal80ts* transgene and were raised at 18°C to inhibit expression of the RNAi transgenes during embryonic and larval development, then shifted to 30°C at 0 hr APF to allow Gal4-mediated induction of the RNAi transgenes during pupal and adult life. Note that although trachea still reach the surface (dashed lines), tracheal invasion is absent in animals with tracheal knockdown of *btl* or muscle knockdown of *bnl*. Scale bars represent 1 μm.

See also Figure S3.

initially evaluated *bnl* and *btl* heterozygotes and a *bnl btl* double heterozygote. All of the mutants showed a reduction in tracheal branches and branch points within muscle fibers, although the effects were most dramatic (60%–75% reduction) in $bnl^{+/-}$ heterozygotes and the $bnl^{+/-}$ $btl^{+/-}$ double heterozygote (Figures 3A and 3B). We also tested the effect of RNAi knockdown of *btl* expression in the tracheal system during pupal development, which completely abrogated flight muscle invasion (Figure 3C). Tracheal expression of a dominant-negative *btl FGFR* construct or the FGF pathway antagonist *sprouty* also reduced flight muscle invasion (Figure S3A), whereas expression of *btl FGFR* RNAi after tracheal invasion (Figure S3B) or using a muscle-specific driver had no effect (Figure 3C). We conclude that Btl FGFR signaling in the trachea is required for flight muscle invasion and is required during the invasion process. Similar experiments with a *bnl* RNAi construct (Figure 3C) demonstrated that Bnl FGF is required in the flight muscle during the same developmental period for tracheal invasion.

Branchless FGF Localizes to T-Tubules during Invasion

Although Bnl FGF can guide outgrowth to individual cells expressing the gene (Jarecki et al., 1999), we sought to understand how it functions in the subcellular targeting of T-tubules during flight muscle invasion. We examined the localization of secreted Bnl FGF protein in flight muscle during pupal development using an antibody staining protocol that detects only extracellular proteins (Figure 4A) (Strigini and Cohen, 2000; Belenkaya et al., 2004). We first validated the specificity of the protocol for Bnl by showing that extracellular immunostaining in flight muscle decreased when endogenous Bnl levels were reduced by RNAi knockdown (Figure S4) and increased when *bnl* was overexpressed (Figures 4D and 4E). Using the validated procedure, we found that there was a developmental shift in Bnl localization. Before invasion, as tracheal branches grew out and ramified on the flight muscle surface, Bnl immunostaining was detected at similar low levels on both the plasma membrane and T-tubules of the flight muscle (Figures 4A and 4B). But as tracheal invasion commenced, Bnl FGF levels increased on the T-tubules and declined on the plasma membrane until they were almost undetectable (Figure 4C). Thus, there is a developmental transition in Bnl FGF localization that coincides with the transition from surface outgrowth to T-tubule invasion.

Bnl Overexpression Leads to Its Surface Accumulation and Increased Surface Branching at Expense of Invasion

Overexpression of Bnl in the flight muscle during tracheal invasion substantially increased the levels of secreted Bnl on both the plasma membrane and the T-tubules, eliminating the normal differential (Figure 4E). Under these conditions, the number of tracheal branches on the muscle surface increased, whereas tracheal invasion of T-tubules was reduced (Figure 4F). By contrast, expression of a constitutively active form of Btl FGFR in trachea during this same period increased both surface branching and invasion (Figure 4F), implying that it was the change in signal distribution and not just increased levels of

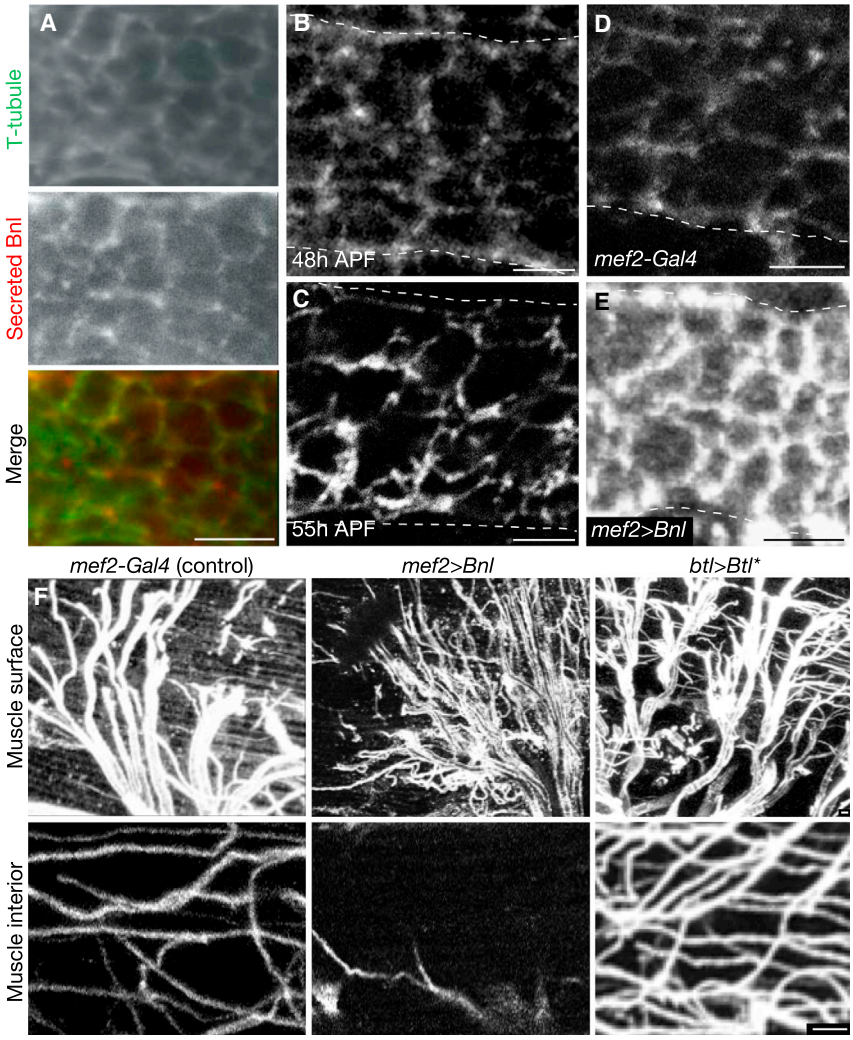

Figure 4. Localized Secretion and Function of Bnl FGF during Tracheal Invasion

(A) Interior view of indirect flight muscle fiber of a *mef2-Gal4*; *UAS-CD8-GFP* pupa at 55 hr APF with native CD8-GFP fluorescence to show T-tubules (green) and immunostaining for Bnl using an extracellular staining protocol to show only secreted Bnl (Secreted Bnl, red). No cytoplasmic staining is detected, unlike standard immunostaining conditions, which detect abundant cytoplasmic Bnl.

(B and C) Secreted Bnl detected as above in indirect flight muscle fiber before (48 hr APF) (B) and during (55 hr APF) (C) tracheal invasion. Animals were prepared and stained in parallel and imaged using identical settings. Note increased levels of secreted Bnl in T-tubules during invasion. Dashed lines, plasma membrane of syncytial muscle fiber.

(D and E) Secreted Bnl detected as above in indirect flight muscle fiber 55 hr APF of control (*mef2-Gal4*) or *mef2-Gal4*; *UAS-bnlA1-1* that overexpresses Bnl in flight muscle. Dotted lines, plasma membrane of flight muscle fiber. Note overexpression results in increased Bnl on both T-tubule and plasma membrane (E) compared to matched control (D).

(F) Effect of Bnl overexpression on tracheal branching on flight muscle. Surface (upper row) and interior views (bottom row) of single muscle fibers immunostained for D3 antigen to show trachea (white) of control (*mef2-Gal4*), *mef2-Gal4*; *UAS-bnlA1-1* adult that overexpresses Bnl FGF in muscle, or *btl-Gal4; UAS-λBtl (btl > Btl*)* adult that expresses a constitutively-active form of Btl FGFR in the tracheal system. Note extensive tracheal branching on flight muscle surface but reduced tracheal invasion following Bnl overexpression and extensive surface branching and invasion associated with constitutively-active Btl expression. Amphiphysin staining showed normal structure and distribution of T-tubules under these conditions. Scale bars represent 1 μm.

See also Figure S4.

signaling that was responsible for the difference. We conclude that tracheal invasion depends on the selective localization of Bnl to T-tubules and its depletion from the muscle surface.

Some Basolateral Epithelial Membrane Proteins Localize to T-Tubules

To begin to address the mechanism underlying the transition in Bnl distribution from plasma membrane surface to the T-tubule network, we first molecularly characterized the flight muscle plasma membrane (sarcolemma) and T-tubule membrane domains. Although many functional and molecular differences have been identified between mammalian sarcolemma (e.g., postsynaptic neural specializations and costameres linking to the contractile machinery) (Pardo et al., 1983; Bloch et al., 2004) and T-tubule (e.g., excitation-contraction coupling including the dihydropyrimidine receptor) (Curtis and Catterall, 1983; Fosset et al., 1983; Al-Qusairi and Laporte, 2011) membrane compartments, few markers are known that distinguish these membrane domains in *Drosophila* (marked with * in Figure 5G). One of the two canonical *Drosophila* T-tubule markers is Discs large (DLG) (Figure 5A) (Thomas et al., 2000; Razzaq et al., 2001), the prototypical membrane-associated guanylate kinase (MAGUK), that localizes in polarized epithelia to septate junctions encompassing much of the lateral cell surface and is required for septate junction formation and basolateral membrane identity (Laprise and Tepass, 2011). During tracheal invasion, DLG was broadly localized to both the plasma membrane and T-tubules (Figures 5B–5E), although localization restricts to the T-tubules in mature *Drosophila* flight muscle (Figure 5A) (Razzaq et al., 2001).

We examined the expression and distribution in developing flight muscle of septate junction and basolateral identity proteins and found four additional proteins that localized specifically or preferentially to T-tubules during tracheal invasion. These include Scribble (Scrib) (Figure 5E), another key component of the Scribble/Discs large (DLG)/Lethal (2) giant larvae (LGL) basolateral identity complex (Figure 5H, "Scrib module") and Na^+,K^+ ATPase α (Figure 5F), a component of the other basolateral identity complex in *Drosophila* (Figure 5H, "Yurt/Coracle group") that also localizes to septate junctions (Laprise and Tepass, 2011), as

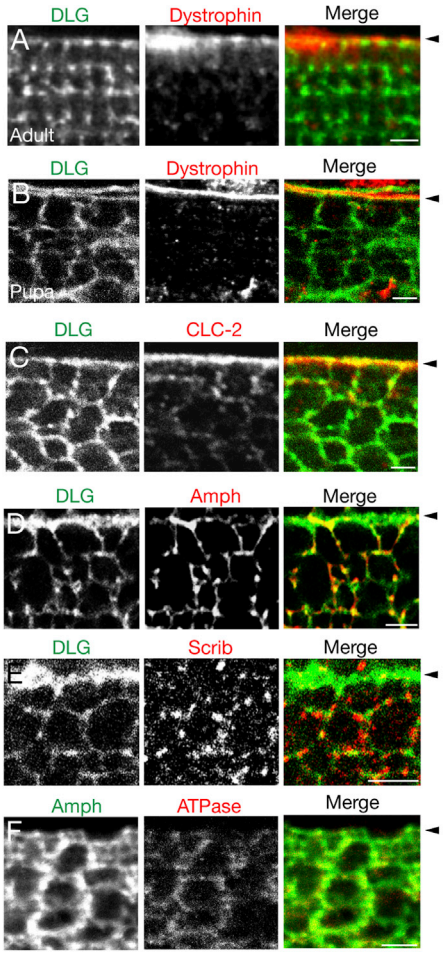

G

Marker	Fl. muscle		Epithelium			Ref
	T-tub	PM	Lat/SJ	Ap	Bas	
Amph/BIN1*	+	-	?	?	?	1
DLG*	+	(+)	Scrib	-	-	1,2
Scribble	+	-	Scrib	-	-	2
Na/K ATPase	+	-	Yurt	-	-	3,4
Neuroglian	+	-	+	-	-	3,5
Fasciclin 3	+	-	+	-	-	6
Dystrophin*	-	+	-	-	-	7,8
CLC-2	+/-	+	?	+	+	9,10
Dystroglycan*	-	+	-	-	+	7,8,11
β-PS Integrin*	-	+	-	-	+	11,12,13
Coracle	-	-	Yurt	-	-	4
Neurexin IV	-	-	Yurt	-	-	4
PAR6	-	-	-	Par	-	14,15,17
Bazooka	-	-	-	Par	-	16,17
aPKC	-	-	-	Par	-	16,17
Crumbs	-	-	-	Crb	-	17,18
Stardust	-	-	-	Crb	-	17,18
PATJ	-	-	-	Crb	-	17,18
α-Catenin	+	-	-	Cad	-	19
β-Catenin	+/-	+	-	Cad	-	19

H

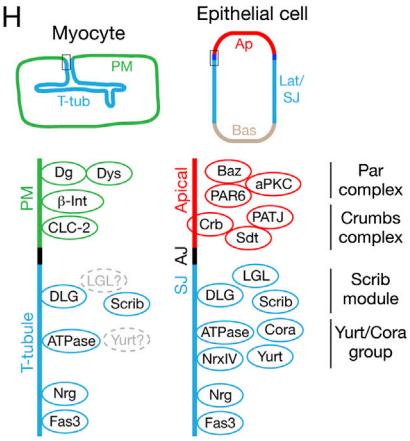

Figure 5. Flight Muscle T-Tubules Express Epithelial Basolateral Markers

(A–F) Interior views of indirect flight muscle fiber of *mefl-Gal4*; *UAS-CD8-GFP* adult (A) and 55 hr APF pupae (B–F) immunostained for the indicated proteins. Arrowheads, position of fiber plasma membrane. (A) Discs large (DLG), part of Scribble/DLG/LGL epithelial basolateral identity module, localizes to adult flight muscle T-tubules. Dystrophin localizes to plasma membrane. (B) During tracheal invasion, DLG localizes to both plasma membrane and T-tubules. (C) Chloride channel CLC-2 localizes to plasma membrane. (D) Amphiphysin localizes to T-tubules. (E) Scribble, another component of Scribble/DLG/LGL basolateral identity module, localizes to puncta associated with T-tubules but not with plasma membrane. (F), Na^+,K^+ ATPase α (ATPase), a component of Yurt/Coracle basolateral identity group in *Drosophila*, localizes to T-tubules.

(G) Summary of T-tubule and sarcolemma markers during tracheal invasion. *Marker with previously known muscle localization in *Drosophila*. +, marker localizes to the indicated membrane domain (T-tub, T-tubule; PM, plasma membrane [sarcolemma]); +/−, marker localizes to indicated membrane domain at lower levels; (+), marker localizes to indicated membrane domain during pupal development, but not in adult tissue. Localization of marker protein in epithelia (Lat/SJ, basolateral/septate junction; Ap, apical; Bas, basal) are indicated by either a + or the name of the complex they are part of (Scrib, Scribble module; Yurt, Yurt/Coracle group; Par, Par complex; Crb, Crumbs complex; Cad, Cadherin complex). Ref, references for epithelial staining and muscle markers indicated by asterisks. Reference 1, Razzaq et al. (2001); 2, Bilder and Perrimon (2000); 3, Laprise et al. (2009); 4, Mohler et al. (2005); 5, Genova and Fehon (2003); 6, Woods et al. (1997); 7, Rybakova et al. (2000); 8, Bogdanik et al. (2008); 9, Peña-Münzenmayer et al. (2005); 10, Blaisdell et al. (2000); 11, Ribeiro et al. (2011); 12, Deng et al. (2003); 13, Fernández-Miñán et al. (2007); 14, Rolls et al. (2003); 15, Petronczki and Knoblich (2001); 16, Schober et al. (1999); 17, Tanentzapf and Tepass (2003); 18, Bulgakova and Knust (2009); 19, McGill et al. (2009).

(H) Schematic comparing localization of membrane domain markers at the indicated region (box) of flight muscle myocyte (left) and polarized epithelial cell (right), focusing on myocyte plasma membrane (sarcolemma [SL], green), T-tubule domain (blue), apical epithelial membrane (red), adherens junction (AJ, black), and septate junction (SJ, blue). Components of epithelial polarity complexes are clustered with names of the complex indicated at right. Proteins in gray, not determined. Scale bars represent 2 μm.

See also Figure S5.

well as Neuroglian (Nrg) (Figure S5A) and Fasciclin 3 (Fas3), transmembrane proteins localized at or near septate junctions that depend on these complexes (Genova and Fehon, 2003; Laprise et al., 2009) for their proper lateral membrane distribution. Thus, the developing flight muscle T-tubule membranes comprise a membrane domain with molecular features in common with lateral epithelial membranes and specifically the septate junction (Figures 5G and 5H). However, T-tubule membranes are not identical to epithelial lateral membranes or septate junctions as several tested members of these complexes were either not expressed in muscle (e.g., Coracle and Neurexin IV) or did not specifically localize to T-tubules (Figures 5G, 5H, and S5B).

We also searched for specific markers of the flight muscle plasma membrane during tracheal invasion. We examined apical epithelial identity complexes and markers and found that they were either not expressed (members of the Crumbs complex [Crumbs, Stardust, PATJ]) or expressed but not specifically localized to any obvious membrane domain (Par complex [PAR6, Bazooka, and aPKC]) (Figures 5G, 5H, and S5C). Four markers (dystrophin, CLC-2, dystroglycan, β_{PS}-integrin) were found that specifically labeled the flight muscle sarcolemma (Figures 5B, 5C, and 5G), two of which (dystroglycan, β_{PS}-integrin) also label the basal membrane domain of polarized epithelia in *Drosophila* (Ayalon et al., 2011; Ribeiro et al., 2011).

AP-1 Knockdown Reroutes Bnl Secretion and Tracheal Growth to the Myocyte Surface

The T-tubule localization of Bnl observed during invasion might arise from targeted secretion of the protein to T-tubule

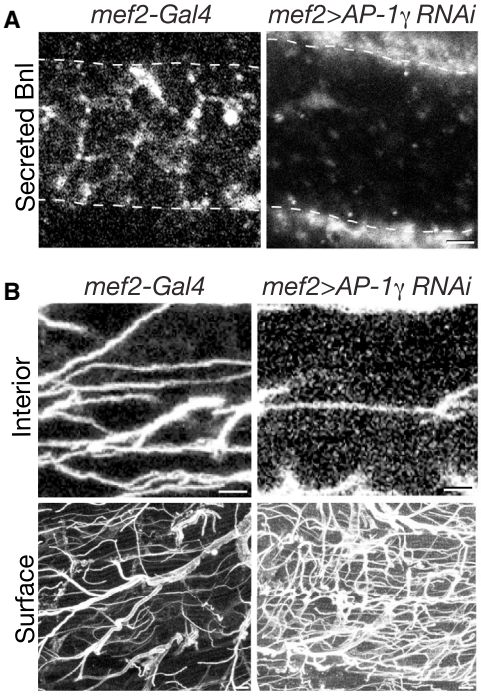

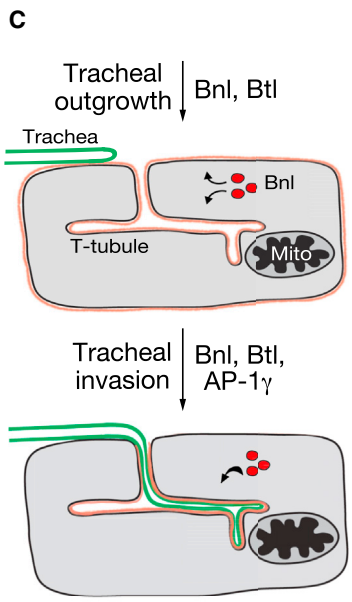

Figure 6. Effect of Knockdown of Clathrin Adaptor AP-1γ on Bnl Localization and Tracheal Invasion of Flight Muscle

(A and B) Indirect flight muscle fibers of control (left, *mef2-Gal4*) and muscle-specific AP-1γ knockdown (right, *mef2-Gal4*; *UAS-CD8::GFP/UAS-AP-1γ RNAi*) pupal (A) and adult (B) *Drosophila* immunostained as in Figure 4A to show secreted Bnl (A, white) or immunostained for D3 antigen (white) to show tracheal invasion (B). Note severely reduced T-tubule localization and increased surface localization of Bnl (A) and almost complete abrogation of tracheal invasion and increased surface ramification (B) in AP-1γ knockdown. Dashes, edge of muscle fiber. Scale bars represent 1 μm (A, upper panel in B), 5 μm (lower panel in B).

(C) Model of AP-1-dependent Bnl localization and tracheal invasion of flight muscle. Top: Bnl FGF (red) is secreted at similar levels at plasma membrane and T-tubule membranes of flight muscle, attracting tracheal branches to the tissue. Bottom: an AP-1γ-dependent developmental switch promotes Bnl FGF secretion at T-tubules, causing tracheal invasion.

See also Figure S6.

membranes. Although many markers localize selectively to T-tubule membranes in mammalian myocytes and *Drosophila* flight muscle (see above), it is unclear how cargoes are specifically delivered there. Given the molecular parallels identified above between T-tubules and epithelial lateral domains and septate junctions, we investigated the effect of flight-muscle-specific knockdown of genes implicated in basolateral secretion. Knockdown of one of them, AP-1γ, a component of the AP-1 clathrin adaptor complex, had a selective and striking effect, as detailed below.

Clathrin and the Clathrin AP-1 adaptor complexes have been implicated in secretion and trafficking to basolateral domains from recycling endosomes and/or the *trans*-Golgi network (TGN) in mammalian (Gan et al., 2002; Traub and Apodaca, 2003; Icking et al., 2007; Guo et al., 2013; Rodriguez-Boulan et al., 2013) and *Drosophila* epithelia (Peng et al., 2009; Benhra et al., 2011); there is a single AP-1 complex in *Drosophila* and two in mammals. Knockdown of expression of the AP-1γ subunit in *Drosophila* salivary glands (Peng et al., 2009) or sensory organ precursors (Benhra et al., 2011) leads to rerouting of basolateral-directed cargo to the apical membrane domain. We found that muscle-specific knockdown of the AP-1γ subunit (*mef2-Gal4* > AP-1γ [RNAi]) during pupal development led to a dramatic rerouting of Branchless from the T-tubules, where it specifically accumulated in wild-type flight muscle, to the surface of the developing flight muscle (Figure 6A). The structure of the T-tubules as assayed by membrane GFP and amphiphysin localization during invasion and in the adult flight muscles appeared unaffected by AP-1γ knockdown (Figure S6A), and T-tubules remained accessible to 2 mDa dextran during tracheal invasion (Figure S6B). Furthermore, T-tubule markers amphiphysin and DLG showed their normal T-tubule localization in adult flight muscles (Figure S6A). We conclude that the clathrin adaptor AP-1γ is required for the selective targeting of Bnl FGF to flight muscle T-tubules, and in its absence Bnl FGF is secreted at the plasma membrane.

Under the same knockdown conditions, we observed an equally dramatic effect on tracheal invasion. There were few or no invading trachea in AP-1γ-depleted flight muscle fibers (Figure 6B), but many more branches than normal on the flight muscle surface (Figure 6B). Thus, although tracheal branches could grow toward and ramify on the flight muscle surface, tracheal projections were unable to invade the T-tubule network. We conclude that AP-1γ is required for both T-tubule Bnl localization and tracheal invasion.

DISCUSSION

The results presented here on *Drosophila* flight muscle development demonstrate that, in addition to the well-established role of developmental control of *bnl* expression in defining the timing and pattern of tracheal branch budding and outgrowth to target tissues (Sutherland et al., 1996; Jarecki et al., 1999; Sato and Kornberg, 2002; Weaver and Krasnow, 2008; Chen and Krasnow, 2014), developmental control of the specific site of Bnl FGF secretion by a target cell can direct terminal branches to sites within the cell where oxygen is needed. In developing flight muscle, we found that tracheae initially grow out and ramify on its surface, just like in other tissues. Subsequently, fine terminal branches invade the T-tubule network, entering through ~300 nm surface openings. As invasion begins, there is a switch in Bnl FGF distribution from a broad localization across the myocyte membrane, attracting tracheae to the muscle, to a selective T-tubule localization. This developmental switch in

Bnl distribution is critical as knockdown or inhibition of Bnl or its receptor Btl during invasion blocks the process, whereas overexpression of Bnl in flight muscle to restore uniform surface and T-tubule distribution promotes surface branching and inhibits invasion. We further showed that T-tubule membranes are specialized domains distinguished by localization of several core regulators of epithelial basolateral membrane identity, and knockdown of the AP-1γ clathrin adaptor implicated in basolateral trafficking prevented the T-tubule accumulation of Bnl FGF and shunted it to the surface, promoting surface branching at the expense of tracheal invasion. The results support a model in which tracheal invasion of flight muscle is controlled by a developmental switch in the subcellular localization of Bnl FGF (Figure 6C). This switch is mediated by AP-1-dependent trafficking of Branchless FGF to the T-tubules, where the ligand attracts tracheae from the surface into the T-tubule network and ultimately to the mitochondria where oxygen is utilized.

Targeting Branchless FGF to T-Tubules

Plasma membrane (sarcolemma) and T-tubule membranes of myocytes have long been known to be molecularly and functionally distinct (Al-Qusairi and Laporte, 2011), and studies of viral protein trafficking demonstrate that these membrane domains can be targeted separately (Rahkila et al., 2001). However, how these membrane domains are established and how endogenous proteins are selectively targeted and retained is unknown. Our findings that several core components of the epithelial DLG/Scrib/LGL basolateral polarity module preferentially mark the T-tubule membrane domain (Figure 5G), and the AP-1γ clathrin adaptor implicated in basolateral trafficking promotes targeting of Bnl to these membranes and away from the sarcolemma provide an entry to these questions. Perhaps AP-1 is involved in sorting Bnl at the trans-Golgi network (TGN) or trafficking or recycling of Bnl-containing vesicles to the T-tubule membrane (Figure 6C), similar to the role proposed for mammalian AP-1 in polarized secretion to epithelial basolateral membrane domains (Gan et al., 2002; Traub and Apodaca, 2003; Ickng et al., 2007; Guo et al., 2013; Rodriguez-Boulan et al., 2013). The localization of other T-tubule proteins examined was not affected by AP-1γ knockdown (Figure S6C), so AP-1-mediated trafficking to T-tubules appears selective and not crucial for maintaining T-tubule identity. Our results also imply that AP-1γ is dispensable for trafficking Bnl to the sarcolemma, because Bnl selectively accumulates there following AP-1γ knockdown. It will be important to elucidate the AP-1-dependent T-tubule targeting pathway and other membrane trafficking pathways in myocytes, as well as to identify the developmental signal that activates the AP-1 complex to ensure the timely change in Bnl localization and the switch from surface branching to tracheal invasion before the onset of flight.

Although our results provide only an initial view of the T-tubule targeting pathway, already several parallels are apparent to the well-studied pathway controlling basolateral domains in polarized epithelial cells (Figure 5H). Previous studies of vesicular stomatitis virus glycoprotein showed that this glycoprotein targets both the basolateral domains of mammalian epithelial cells and the T-tubule network of skeletal muscle (Rahkila et al., 2001), suggesting a functional parallel. Our finding that multiple proteins in the core DLG/Scrib/LGL basolateral polarity module preferentially mark the T-tubule membrane provide molecular support for this view, and the parallel functions of AP-1 in T-tubule trafficking and basolateral targeting in polarized epithelia further support this idea. However, a number of key basolateral trafficking proteins are not detectably expressed in flight muscle or do not localize to T-tubules (Figures 5G and 5H), demonstrating important differences as well. We found little, if any, correspondence between sarcolemma and apical epithelial markers, implying a separate mechanism for establishing the sarcolemma domain. Thus, it appears that membrane trafficking in muscle cells has adopted some of the molecules and mechanisms of epithelial basolateral targeting, just as neurons appear to have done for sorting of specific cargos to dendrites (Jareb and Banker, 1998; Margeta et al., 2009).

T-Tubule Transitions during Tracheal Invasion

In addition to the transition in Bnl localization at the time of invasion, we discovered two other notable transitions of flight muscle T-tubules associated with invasion. First, T-tubule surface openings dilate to ~30 times their normal size, expanding to 300 nm diameter or more (Figure 1H), large enough to allow entry of filopodia (100–300 nm) (Zhuravlev and Papoian, 2009). This expansion is transient as just 40 hr after tracheal invasion has begun, the large openings are no longer detected and flight muscle T-tubules narrow to a size similar to those in pupal tubular muscles and flight muscle in the adult (Razzaq et al., 2001). T-tubules of other muscles examined did not undergo dilation, implying that T-tubule dilation is a flight-muscle-specific innovation. Second, by 70 hr APF when invasion is complete, the invaded T-tubules show a different marker expression pattern, losing localization of T-tubule molecular markers such as amphiphysin (Figure S1A). Thus, the T-tubule developmental program has apparently specialized to accommodate invasion of tracheal branches that feed the tissue's extreme oxygen demand.

Other Guidance Factors in Tracheal Invasion

Although the results demonstrate that Bnl FGF plays a decisive role in tracheal invasion, it is unlikely to be the only signal. Bnl is distributed rather uniformly across the T-tubule network during invasion, yet tracheae invade only a subset of T-tubules, making dramatic turns (such as abrupt 90° turns immediately after entry) before reaching their targets. We presume that other guidance cues function with Bnl to specify the tracheal outgrowth path within the T-tubule network. A priority for future work is to identify the signal that controls the specific pathway that terminal branches traverse within the T-tubule network that ends in encircling the mitochondria (Wigglesworth and Lee, 1982) and hence oxygen delivery directly to the organelle that uses it. Such targeting would presumably require even more precise subcellular signal localization, to the T-tubules abutting mitochondria.

Although most growth factors and chemoattractants are presumed to be secreted quite generally from the source cells, some that are expressed in polarized epithelial cells have been shown to be selectively secreted from apical or basolateral domains, typically from the domain closest to the receiving cells (Strigini and Cohen, 2000; Rosin et al., 2004). Growth factors

and chemoattractants have also been found to be localized to or secreted from specific membrane domains of neurons, such as dendritic targeting of brain-derived neurotrophic factor (BDNF) and localization of Neurofascin186 at the initial segment of Purkinje cell axons to guide advancing basket cells (Ango et al., 2004). It will be important to explore how broadly important subcellular targeting of secretion and accumulation of growth factors and chemoattractants is and whether T-tubule targeting of Bnl FGF and entry into the target cell represents an extreme example of a more general class of regulatory mechanisms, with extravagant morphogenetic consequences serving a critical physiological role.

EXPERIMENTAL PROCEDURES

Drosophila Strains and Genetics

bnl^{P1} (Sutherland et al., 1996) and btl^{LG18} (Klämbt et al., 1992) are null alleles. The Gal4/UAS system (Brand et al., 1994) was used, with *btl-Gal4* (Ohshiro and Saigo, 1997) used to drive tracheal expression of transgenes and *mef2-Gal4* (Ranganayakulu et al., 1995) used to drive muscle expression. *tubulin-Gal80ts* (McGuire et al., 2004) encodes a ubiquitously expressed and temperature-sensitive repressor of Gal4 activity. UAS responders were: *UAS-DNbtl* (dominant-negative Btl) (Reichman-Fried et al., 1994), *UAS-btl-RNAi* (transformant ID 950, Vienna *Drosophila* RNAi Center (VDRC), Dietzl et al., 2007), *UAS-λbtl* (constitutively-active Btl) (Anderson et al., 1996), *UAS-bnl-RNAi* (transformant ID 5730, VDRC), *UAS-bnlA1-1* (wild-type Bnl) (Sutherland et al., 1996), *UAS-spry* (Hacohen et al., 1998), *UAS-AP-1γ-RNAi* (line ID JF02684, Transgenic RNAi Project [TRiP]), and *UAS-CD8-GFP* (Lee and Luo, 1999). Crosses were done at 25°C unless noted otherwise.

Temporal Expression of Transgenes

The *btl-Gal4* driver was used with *tubulin-Gal80ts*, a Gal80 temperature-sensitive repressor, to temporally restrict tracheal expression of *UAS-spry*, *UAS-DNbtl*, *UAS-λbtl*, and *UAS-btl-RNAi* responders to the pupal tracheal system: *btl-Gal4*, *UAS-GFP/ tubulin-Gal80ts*; *btl-Gal4*, *UAS-GFP/ UAS-DNbtl* (or *UAS-λbtl*, *UAS-DNbtl*, *UAS-spry*, or *UAS-btl-RNAi*) flies were grown at 18°C until 0 hr APF, then shifted to 30°C to inactivate Gal80ts and allow Gal4-mediated induction of transgenes. To temporally deplete Bnl FGF by RNAi, *mef2-Gal4*; *tubulin-Gal80ts/ UAS-Bnl-RNAi* flies were treated in the same way.

Labeling of Tracheal Clones

For clonal marking of tracheal cells, the MARCM system (Lee and Luo, 1999) was used. Two- to 6-hour-old *y w hs-flp*^{122}*; FRT40A, FRTG13, btl-Gal4, UAS-GFP/FRTG13 tubulin-Gal80* embryos raised at 25°C were placed at 38°C for 45 min to induce sporadic GFP-labeled tracheal cells. Animals were returned to 25°C to continue development and analyzed as described below.

Immunostaining and Fluorescence Microscopy

Animals were examined during pupal development for staging and then analyzed at the indicated time after puparium formation (APF). Pupae were immersed in chilled PBS (pH 7.4) and then mounted with pins and dissected along the ventral midline with transverse cuts at the anterior and posterior to allow access to the flight muscles. Animals were then fixed for 25 min at room temperature in 4% paraformaldehyde (PFA)/PBS and washed in PBS. Adults were dissected 1–3 days following eclosion. Animals were flash frozen in liquid nitrogen and then bisected at the dorsal midline with a blade. Hemithoraces were placed directly into chilled 4% PFA/PBS and fixed for 25 min at room temperature.

For both pupal and adult preparations, antigen blocking was done at room temperature for 30 min in PBS with 0.1% Triton X-100 (PBST), and subsequent incubations were conducted in PBST. Primary antibody incubations were done at 4°C overnight. Antibodies were: chicken anti-GFP (Abcam; 1:500), mouse anti-Complex 5, alpha subunit (Mitosciences, 1:250), rabbit anti-amphiphysin (1:500) (Razzaq et al., 2001), mouse mAb68G5D3 (abbreviated "D3") (1:10) (Giniger et al., 1993), mouse anti-Discs large (4F3, Developmental Studies Hybridoma Bank [DSHB]; 1:10), mouse anti-ATPase, (Na^+, K^+ alpha subunit) (a5, DSHB; 1:100), rabbit anti-Scribble (1:500) (Bilder and Perrimon, 2000), rat anti-alpha-Catenin (DCAT-1, DSHB; 1:100), rabbit anti-dystrophin CO2H (1:1,000) (van der Plas et al., 2006); mouse anti-Armadillo (N2 7A1, DSHB; 1:100), rat anti-PAR6 (1:200) (Rolls et al., 2003), mouse anti-Neuroglian (BP 104, DSHB; 1:100), and mouse anti-Syntaxin (8C3, DSHB; 1:100). Fluorescent secondary antibodies (Jackson Immunoresearch) were used at 1:250. DAPI (100 ng/ml) was used to stain nuclei.

To detect extracellular Bnl FGF, we used an extracellular immunostaining protocol in which the specimen is incubated with primary antiserum and washed before fixation (Strigini and Cohen, 2000; Belenkaya et al., 2004). Pupae were dissected on ice in chilled Schneider's M3 media (Sigma) and then incubated with preabsorbed, protein A-purified rabbit anti-Bnl antiserum (Sutherland et al., 1996; Jarecki et al., 1999) (1:20 in M3) for 45 min on ice. After washing with ice cold PBS three times for 90 s, preparations were fixed for 30 min in ice cold 4% PFA/PBS, washed, then processed for immunostaining as above. Experimental specimens were dissected and stained in parallel with control pupae.

Stained specimens were analyzed by confocal fluorescence microscopy (Leica SP2 AOBS). All images shown of individual flight muscle fibers are 10 μm compressed stacks taken ~20–50 μm below the flight muscle surface, except when noted as "muscle surface" images. Boundaries of individual muscle fibers were identified by immunostaining of amphiphysin and the localization of F-actin filaments as visualized by phalloidin (Molecular Probes) staining. The number of branches and branch points per muscle fiber was assessed by counts of invaded D3-labeled tracheal branches, or branch points, in randomly selected 10 μm compressed stacks of adult flight muscle fibers.

Scanning Electron Microscopy

mef2-Gal4 leg tubular and flight muscles were dissected at the indicated times and fixed overnight at 4°C in 4% paraformaldehyde in PBS (pH 7.4). Muscles were then postfixed in 1% osmium tetroxide and stained with 2% uranyl acetate in deionized water for 15 min. Muscles were critical-point dried and sputter-coated with gold by standard methods (Stanford Electron Microscopy Core) and imaged with a scanning electron microscope (Hitachi S-3400N VP-SEM).

T-Tubule Accessibility Assay

Accessibility of T-tubules in AP-1γ knockdown and in wild-type pupae was evaluated by incubating freshly dissected *mef2-Gal4/UAS-CD8-GFP*; *UAS-AP-1γ* pupa with 2 mg/ml lysine-fixable 2,000,000 MW or 500,000 MW dextran conjugated to tetramethylrhodamine in ice cold PBS (Molecular Probes) for 20 min. Preparations were immediately fixed for 30 min at room temperature, washed three times in PBS for 5 min, and immediately imaged by confocal microscopy. All steps after addition of dextran were protected from light.

SUPPLEMENTAL INFORMATION

Supplemental Information includes six figures and can be found with this article online at http://dx.doi.org/10.1016/j.cell.2014.11.043.

ACKNOWLEDGMENTS

We thank Drs. Suzanne Pfeffer, Nipam Patel, James Nelson, and laboratory members for helpful discussions and Drs. Eric Olson, Cahir O'Kane, David Bilder, Jasprien Noordermeer, and Chris Doe for reagents. Figure S2 and the Graphical Abstract were adapted from Hartenstein (1993). This work was supported by a Stanford Graduate Fellowship and an American Heart Association Predoctoral Fellowship (S.J.P.) and the Howard Hughes Medical Institute.

Received: July 24, 2014
Revised: October 7, 2014
Accepted: November 15, 2014
Published: December 31, 2014

REFERENCES

Al-Qusairi, L., and Laporte, J. (2011). T-tubule biogenesis and triad formation in skeletal muscle and implication in human diseases. Skelet Muscle *1*, 26.

Anderson, M.G., Certel, S.J., Certel, K., Lee, T., Montell, D.J., and Johnson, W.A. (1996). Function of the Drosophila POU domain transcription factor drifter as an upstream regulator of breathless receptor tyrosine kinase expression in developing trachea. Development *122*, 4169–4178.

Ango, F., di Cristo, G., Higashiyama, H., Bennett, V., Wu, P., and Huang, Z.J. (2004). Ankyrin-based subcellular gradient of neurofascin, an immunoglobulin family protein, directs GABAergic innervation at Purkinje axon initial segment. Cell *119*, 257–272.

Ayalon, G., Hostettler, J.D., Hoffman, J., Kizhatil, K., Davis, J.Q., and Bennett, V. (2011). Ankyrin-B interactions with spectrin and dynactin-4 are required for dystrophin-based protection of skeletal muscle from exercise injury. J. Biol. Chem. *286*, 7370–7378.

Belenkaya, T.Y., Han, C., Yan, D., Opoka, R.J., Khodoun, M., Liu, H., and Lin, X. (2004). *Drosophila* Dpp morphogen movement is independent of dynamin-mediated endocytosis but regulated by the glypican members of heparan sulfate proteoglycans. Cell *119*, 231–244.

Benhra, N., Lallet, S., Cotton, M., Le Bras, S., Dussert, A., and Le Borgne, R. (2011). AP-1 controls the trafficking of Notch and Sanpodo toward E-cadherin junctions in sensory organ precursors. Curr. Biol. *21*, 87–95.

Bilder, D., and Perrimon, N. (2000). Localization of apical epithelial determinants by the basolateral PDZ protein Scribble. Nature *403*, 676–680.

Blaisdell, C.J., Edmonds, R.D., Wang, X.T., Guggino, S., and Zeitlin, P.L. (2000). pH-regulated chloride secretion in fetal lung epithelia. Am. J. Physiol. Lung Cell. Mol. Physiol. *278*, L1248–L1255.

Bloch, R.J., Reed, P., O'Neill, A., Strong, J., Williams, M., Porter, N., and González-Serratos, H. (2004). Costameres mediate force transduction in healthy skeletal muscle and are altered in muscular dystrophies. J. Muscle Res. Cell Motil. *25*, 590–592.

Bogdanik, L., Framery, B., Frölich, A., Franco, B., Mornet, D., Bockaert, J., Sigrist, S.J., Grau, Y., and Parmentier, M.L. (2008). Muscle dystroglycan organizes the postsynapse and regulates presynaptic neurotransmitter release at the *Drosophila* neuromuscular junction. PLoS ONE *3*, e2084.

Brand, A.H., Manoukian, A.S., and Perrimon, N. (1994). Ectopic expression in *Drosophila*. Methods Cell Biol. *44*, 635–654.

Bulgakova, N.A., and Knust, E. (2009). The Crumbs complex: from epithelial-cell polarity to retinal degeneration. J. Cell Sci. *122*, 2587–2596.

Cajal, S.R.y. (1890). Coloration par la méthode de Golgi des terminaisons des trachées et des nerfs dans les muscles des ailes des insectes. Z. Wissensch. Mikr. (7), 332–342.

Chen, F., and Krasnow, M.A. (2014). Progenitor outgrowth from the niche in *Drosophila* trachea is guided by FGF from decaying branches. Science *343*, 186–189.

Curtis, B.M., and Catterall, W.A. (1983). Solubilization of the calcium antagonist receptor from rat brain. J. Biol. Chem. *258*, 7280–7283.

Deng, W.M., Schneider, M., Frock, R., Castillejo-Lopez, C., Gaman, E.A., Baumgartner, S., and Ruohola-Baker, H. (2003). Dystroglycan is required for polarizing the epithelial cells and the oocyte in *Drosophila*. Development *130*, 173–184.

Dietzl, G., Chen, D., Schnorrer, F., Su, K.C., Barinova, Y., Fellner, M., Gasser, B., Kinsey, K., Oppel, S., Scheiblauer, S., et al. (2007). A genome-wide transgenic RNAi library for conditional gene inactivation in *Drosophila*. Nature *448*, 151–156.

Dreher, M.R., Liu, W., Michelich, C.R., Dewhirst, M.W., Yuan, F., and Chilkoti, A. (2006). Tumor vascular permeability, accumulation, and penetration of macromolecular drug carriers. J. Natl. Cancer Inst. *98*, 335–344.

Dutta, D., Anant, S., Ruiz-Gomez, M., Bate, M., and VijayRaghavan, K. (2004). Founder myoblasts and fibre number during adult myogenesis in *Drosophila*. Development *131*, 3761–3772.

Fernández-Miñán, A., Martín-Bermudo, M.D., and González-Reyes, A. (2007). Integrin signaling regulates spindle orientation in *Drosophila* to preserve the follicular-epithelium monolayer. Curr. Biol. *17*, 683–688.

Fosset, M., Jaimovich, E., Delpont, E., and Lazdunski, M. (1983). [3H]nitrendipine receptors in skeletal muscle. J. Biol. Chem. *258*, 6086–6092.

Gan, Y., McGraw, T.E., and Rodriguez-Boulan, E. (2002). The epithelial-specific adaptor AP1B mediates post-endocytic recycling to the basolateral membrane. Nat. Cell Biol. *4*, 605–609.

Genova, J.L., and Fehon, R.G. (2003). Neuroglian, Gliotactin, and the Na+/K+ ATPase are essential for septate junction function in *Drosophila*. J. Cell Biol. *161*, 979–989.

Giniger, E., Jan, L.Y., and Jan, Y.N. (1993). Specifying the path of the intersegmental nerve of the *Drosophila* embryo: a role for Delta and Notch. Development *117*, 431–440.

Glazer, L., and Shilo, B.Z. (1991). The *Drosophila* FGF-R homolog is expressed in the embryonic tracheal system and appears to be required for directed tracheal cell extension. Genes Dev. *5*, 697–705.

Guo, X., Mattera, R., Ren, X., Chen, Y., Retamal, C., González, A., and Bonifacino, J.S. (2013). The adaptor protein-1 μ1B subunit expands the repertoire of basolateral sorting signal recognition in epithelial cells. Dev. Cell *27*, 353–366.

Hacohen, N., Kramer, S., Sutherland, D., Hiromi, Y., and Krasnow, M.A. (1998). sprouty encodes a novel antagonist of FGF signaling that patterns apical branching of the *Drosophila* airways. Cell *92*, 253–263.

Hartenstein, V. (1993). The Atlas of *Drosophila* Development (Cold Spring Harbor, NY: Cold Spring Harbor Laboratory Press).

Icking, A., Amaddii, M., Ruonala, M., Höning, S., and Tikkanen, R. (2007). Polarized transport of Alzheimer amyloid precursor protein is mediated by adaptor protein complex AP1-1B. Traffic *8*, 285–296.

Jareb, M., and Banker, G. (1998). The polarized sorting of membrane proteins expressed in cultured hippocampal neurons using viral vectors. Neuron *20*, 855–867.

Jarecki, J., Johnson, E., and Krasnow, M.A. (1999). Oxygen regulation of airway branching in *Drosophila* is mediated by branchless FGF. Cell *99*, 211–220.

Klämbt, C., Glazer, L., and Shilo, B.Z. (1992). Breathless, a Drosophila FGF receptor homolog, is essential for migration of tracheal and specific midline glial cells. Genes Dev. *6*, 1668–1678.

Laprise, P., and Tepass, U. (2011). Novel insights into epithelial polarity proteins in *Drosophila*. Trends Cell Biol. *21*, 401–408.

Laprise, P., Lau, K.M., Harris, K.P., Silva-Gagliardi, N.F., Paul, S.M., Beronja, S., Beitel, G.J., McGlade, C.J., and Tepass, U. (2009). Yurt, Coracle, Neurexin IV and the Na(+),K(+)-ATPase form a novel group of epithelial polarity proteins. Nature *459*, 1141–1145.

Lee, T., and Luo, L. (1999). Mosaic analysis with a repressible cell marker for studies of gene function in neuronal morphogenesis. Neuron *22*, 451–461.

Leydig, F. (1859). Zur Anatomic der Insecten (part 2), section 9. Zum Bau der Tracheen. Arch. Anat. Physiol. u Wissensch. Med., 160–162.

Margeta, M.A., Wang, G.J., and Shen, K. (2009). Clathrin adaptor AP-1 complex excludes multiple postsynaptic receptors from axons in *C. elegans*. Proc. Natl. Acad. Sci. USA *106*, 1632–1637.

McGill, M.A., McKinley, R.F., and Harris, T.J. (2009). Independent cadherin-catenin and Bazooka clusters interact to assemble adherens junctions. J. Cell Biol. *185*, 787–796.

McGuire, S.E., Mao, Z., and Davis, R.L. (2004). Spatiotemporal gene expression targeting with the TARGET and gene-switch systems in *Drosophila*. Sci. STKE *2004*, pl6.

Meyer, E.P. (1989). Corrosion casts as a method for investigation of the insect tracheal system. Cell Tissue Res. *256*, 1–6.

Mohler, P.J., Davis, J.Q., and Bennett, V. (2005). Ankyrin-B coordinates the Na/K ATPase, Na/Ca exchanger, and $InsP_3$ receptor in a cardiac T-tubule/SR microdomain. PLoS Biol. *3*, e423.

Ohshiro, T., and Saigo, K. (1997). Transcriptional regulation of breathless FGF receptor gene by binding of TRACHEALESS/dARNT heterodimers to three central midline elements in *Drosophila* developing trachea. Development *124*, 3975–3986.

Pardo, J.V., Siliciano, J.D., and Craig, S.W. (1983). A vinculin-containing cortical lattice in skeletal muscle: transverse lattice elements ("costameres") mark sites of attachment between myofibrils and sarcolemma. Proc. Natl. Acad. Sci. USA *80*, 1008–1012.

Peña-Münzenmayer, G., Catalán, M., Cornejo, I., Figueroa, C.D., Melvin, J.E., Niemeyer, M.I., Cid, L.P., and Sepúlveda, F.V. (2005). Basolateral localization of native ClC-2 chloride channels in absorptive intestinal epithelial cells and basolateral sorting encoded by a CBS-2 domain di-leucine motif. J. Cell Sci. *118*, 4243–4252.

Peng, Y.H., Yang, W.K., Lin, W.H., Lai, T.T., and Chien, C.T. (2009). Nak regulates Dlg basal localization in *Drosophila* salivary gland cells. Biochem. Biophys. Res. Commun. *382*, 108–113.

Petronczki, M., and Knoblich, J.A. (2001). DmPAR-6 directs epithelial polarity and asymmetric cell division of neuroblasts in *Drosophila*. Nat. Cell Biol. *3*, 43–49.

Rahkila, P., Takala, T.E., Parton, R.G., and Metsikkö, K. (2001). Protein targeting to the plasma membrane of adult skeletal muscle fiber: an organized mosaic of functional domains. Exp. Cell Res. *267*, 61–72.

Ranganayakulu, G., Zhao, B., Dokidis, A., Molkentin, J.D., Olson, E.N., and Schulz, R.A. (1995). A series of mutations in the D-MEF2 transcription factor reveal multiple functions in larval and adult myogenesis in *Drosophila*. Dev. Biol. *171*, 169–181.

Razzaq, A., Robinson, I.M., McMahon, H.T., Skepper, J.N., Su, Y., Zelhof, A.C., Jackson, A.P., Gay, N.J., and O'Kane, C.J. (2001). Amphiphysin is necessary for organization of the excitation-contraction coupling machinery of muscles, but not for synaptic vesicle endocytosis in *Drosophila*. Genes Dev. *15*, 2967–2979.

Reichman-Fried, M., Dickson, B., Hafen, E., and Shilo, B.Z. (1994). Elucidation of the role of breathless, a *Drosophila* FGF receptor homolog, in tracheal cell migration. Genes Dev. *8*, 428–439.

Ribeiro, I., Yuan, L., Tanentzapf, G., Dowling, J.J., and Kiger, A. (2011). Phosphoinositide regulation of integrin trafficking required for muscle attachment and maintenance. PLoS Genet. *7*, e1001295.

Rodriguez-Boulan, E., Perez-Bay, A., Schreiner, R., and Gravotta, D. (2013). Response: the "tail" of the twin adaptors. Dev. Cell *27*, 247–248.

Rolls, M.M., Albertson, R., Shih, H.P., Lee, C.Y., and Doe, C.Q. (2003). *Drosophila* aPKC regulates cell polarity and cell proliferation in neuroblasts and epithelia. J. Cell Biol. *163*, 1089–1098.

Rosin, D., Schejter, E., Volk, T., and Shilo, B.Z. (2004). Apical accumulation of the *Drosophila* PDGF/VEGF receptor ligands provides a mechanism for triggering localized actin polymerization. Development *131*, 1939–1948.

Rybakova, I.N., Patel, J.R., and Ervasti, J.M. (2000). The dystrophin complex forms a mechanically strong link between the sarcolemma and costameric actin. J. Cell Biol. *150*, 1209–1214.

Sato, M., and Kornberg, T.B. (2002). FGF is an essential mitogen and chemoattractant for the air sacs of the *Drosophila* tracheal system. Dev. Cell *3*, 195–207.

Schober, M., Schaefer, M., and Knoblich, J.A. (1999). Bazooka recruits Inscuteable to orient asymmetric cell divisions in *Drosophila* neuroblasts. Nature *402*, 548–551.

Smith, D.S. (1961a). Reticular organizations within the striated muscle cell: an historical survey of light microscopic studies. J. Biophys. Biochem. Cytol. *10*, 61–87.

Smith, D.S. (1961b). The structure of insect fibrillar flight muscle: a study made with special reference to the membrane systems of the fiber. J. Biophys. Biochem. Cytol. *10*, 123–158.

Strigini, M., and Cohen, S.M. (2000). Wingless gradient formation in the *Drosophila* wing. Curr. Biol. *10*, 293–300.

Sutherland, D., Samakovlis, C., and Krasnow, M.A. (1996). branchless encodes a *Drosophila* FGF homolog that controls tracheal cell migration and the pattern of branching. Cell *87*, 1091–1101.

Tanentzapf, G., and Tepass, U. (2003). Interactions between the crumbs, lethal giant larvae and bazooka pathways in epithelial polarization. Nat. Cell Biol. *5*, 46–52.

Thomas, U., Ebitsch, S., Gorczyca, M., Koh, Y.H., Hough, C.D., Woods, D., Gundelfinger, E.D., and Budnik, V. (2000). Synaptic targeting and localization of discs-large is a stepwise process controlled by different domains of the protein. Curr. Biol. *10*, 1108–1117.

Traub, L.M., and Apodaca, G. (2003). AP-1B: polarized sorting at the endosome. Nat. Cell Biol. *5*, 1045–1047.

van der Plas, M.C., Pilgram, G.S., Plomp, J.J., de Jong, A., Fradkin, L.G., and Noordermeer, J.N. (2006). Dystrophin is required for appropriate retrograde control of neurotransmitter release at the *Drosophila* neuromuscular junction. J. Neurosci. *26*, 333–344.

Weaver, M., and Krasnow, M.A. (2008). Dual origin of tissue-specific progenitor cells in *Drosophila* tracheal remodeling. Science *321*, 1496–1499.

Weis-Fogh, T. (1961). Power in flapping flight. In The Cell and the Organism, J.A. Ramsay and V.B. Wigglesworth, eds. (London: Cambridge University Press), pp. 283–300.

Weis-Fogh, T. (1964). Diffusion in insect wing muscle, the most active tissue known. J. Exp. Biol. *41*, 229–256.

Wigglesworth, V.B., and Lee, W.M. (1982). The supply of oxygen to the flight muscles of insects: a theory of tracheole physiology. Tissue Cell *14*, 501–518.

Woods, D.F., Wu, J.W., and Bryant, P.J. (1997). Localization of proteins to the apico-lateral junctions of Drosophila epithelia. Dev. Genet. *20*, 111–118.

Zhuravlev, P.I., and Papoian, G.A. (2009). Molecular noise of capping protein binding induces macroscopic instability in filopodial dynamics. Proc. Natl. Acad. Sci. USA *106*, 11570–11575.

Cell

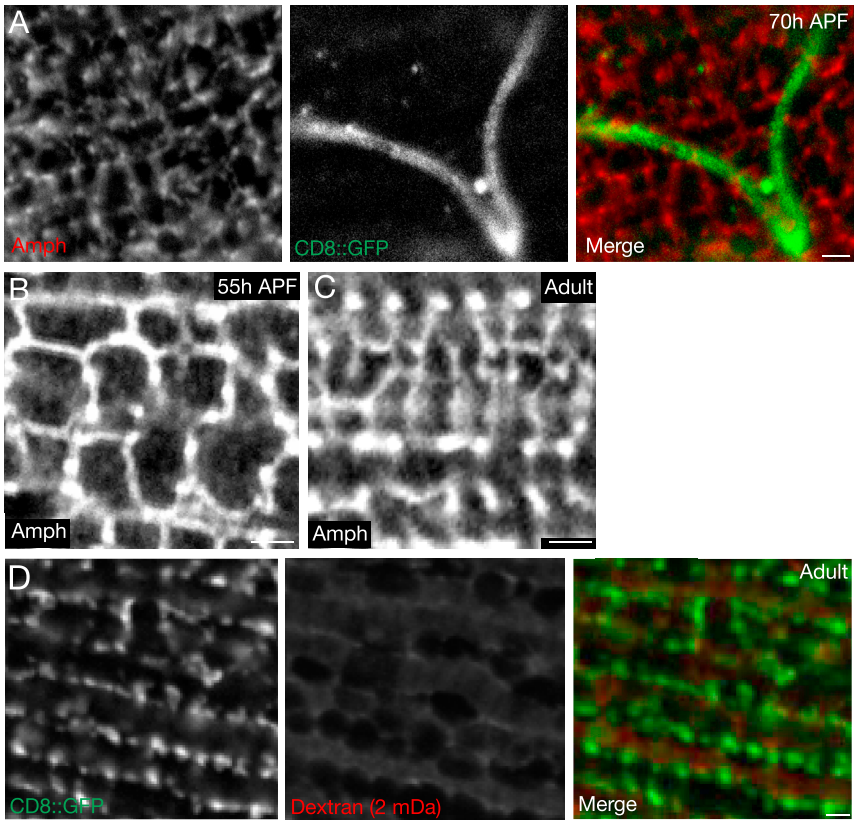

Figure S1. T-Tubule Maturation following Tracheal Invasion, Related to Figure 1

(A) Interior view of indirect flight muscle fiber of *btl-Gal4*; *UAS-CD8::GFP pupa* 70h APF immunostained for amphiphysin (Amph, red) to show T-tubules and for GFP (green) to show tracheal branch that has invaded. Note T-tubule membranes surrounding invaded tracheal branch do not stain for amphiphysin, as they do during the invasion process ~10-15 hr earlier (Figure 1G′).

(B and C) Indirect flight muscle T-tubules immunostained for amphiphysin (white) in pupa at 55h APF during tracheal invasion (B) and in adults (C). T-tubule network is denser but individual T-tubules are narrower in adult.

(D) Indirect flight muscle fiber of adult *mef2-Gal4*; *UAS-CD8::GFP Drosophila* that was incubated with 2 mDa fluorescent dextran (red) for 20 min. No dextran is detectable in T-tubules (GFP fluorescence; green), indicating that adult T-tubules are not accessible as they are during invasion (Figure 1J). Scale bars, 1 μm.

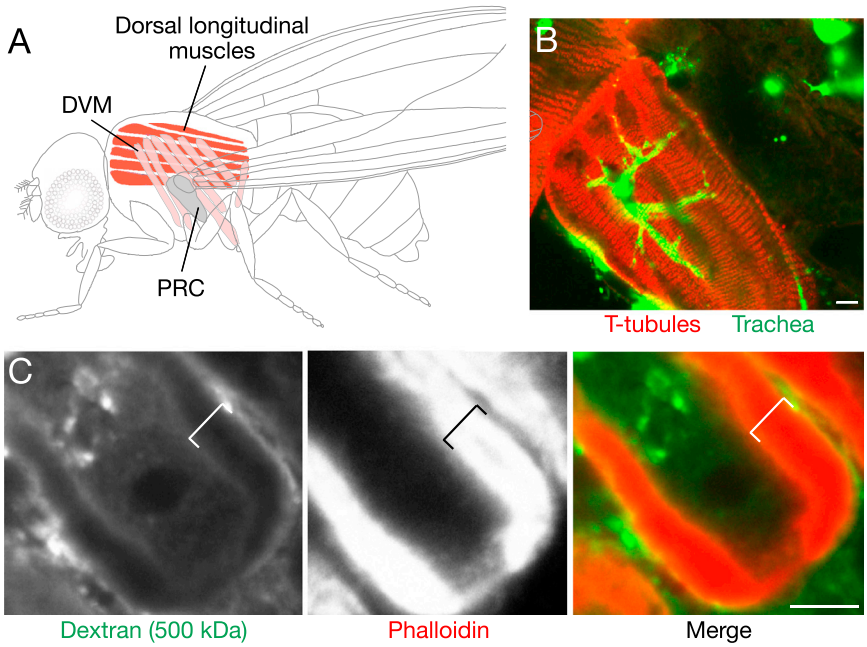

Figure S2. Tubular Muscle T-Tubules Are Not Accessible to Tracheal Projections, Related to Figure 2

(A) Schematic of selected adult *Drosophila* muscles. Red, dorsal longitudinal muscles (DLMs). Gray, plural remotor of coxa (PRC), a tubular muscle. The indirect flight muscle is composed of the DLM and the dorsal ventral muscles (DVM, pink), which are superficial to, and almost perpendicular to, the DLM. Adapted from Hartenstein (1993).

(B) Surface view of plural remotor of coxae muscle of *btl-Gal4; UAS-CD8::GFP* trachea pupa ~64 hr APF immunostained for amphiphysin (red) to show T-tubules and GFP (green) to show tracheae. Tracheal projections extend over the surface and between fibers of this tubular muscle ~15 - 20 hr after tracheal outgrowth to the indirect flight muscle.

(C) Same muscle of 65h APF pupa incubated with fluorescent dextran beads (500 kDa) for 20 min and stained with phalloidin to mark T-tubule region. No dextran is detected in T-tubule region (line), implying that T-tubule openings of this muscle must be less than 15 nm, the estimated diameter of 500 kDa dextrans (Dreher et al., 2006). Scale bars, 2 μm.

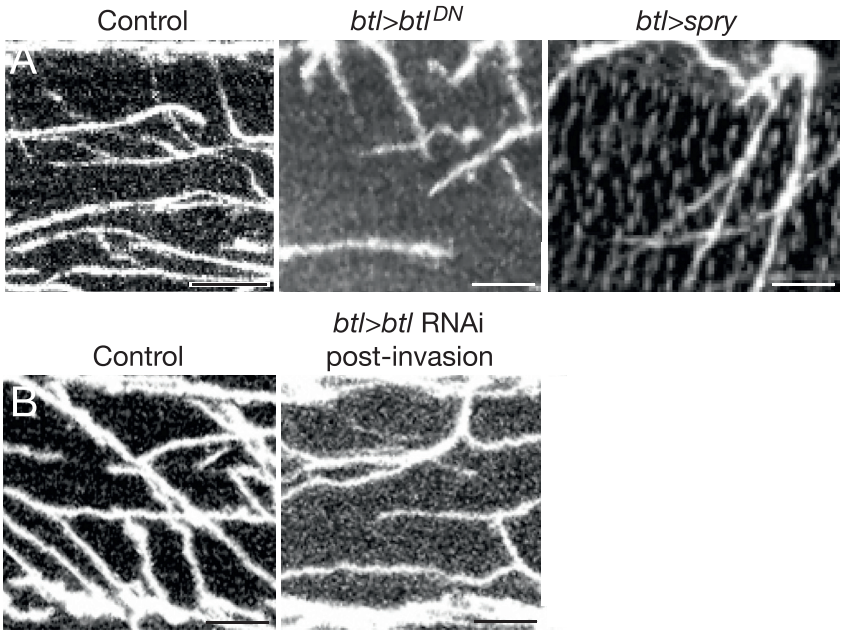

Figure S3. Requirement for Tracheal-Expressed Btl FGFR and Muscle-Expressed Bnl FGF during Invasion, Related to Figure 3

Interior view of adult indirect flight muscle fibers immunostained for D3 tracheal antigen (white) to show tracheal invasion.

(A) Fibers from control (*btl-Gal4*), tracheal-expressed dominant-negative (DN) Btl FGFR (;*btl-Gal4*; *UAS-DN-btl FGFR*) and tracheal-expressed FGF pathway antagonist Sprouty (;*btl-Gal4*; *UAS-spry)*. All animals contained a *tubulin-Gal80ts* transgene and were raised at 18°C to inhibit expression of the UAS transgenes during embryonic and larval development, then shifted to 30°C at 0h APF to allow Gal4-mediated expression of the UAS transgenes during pupal and adult life. Note reduced tracheal invasion by *DN-btl FGFR* or *spry* expression.

(B) Fibers from control (*btl-Gal4*) and *btl* RNAi knockdown (*btl-Gal4*, *UAS-btl-RNAi; UAS-CD8::GFP)* animals as in Figure 3C except that shift to 30°C began at 60h APF (rather than 0h APF) to induce *UAS-btl-RNAi* expression after tracheal outgrowth and invasion of flight muscle. No effect on tracheation was observed, implying that *btl* is not required after outgrowth and invasion. Scale bars, 5 μm.

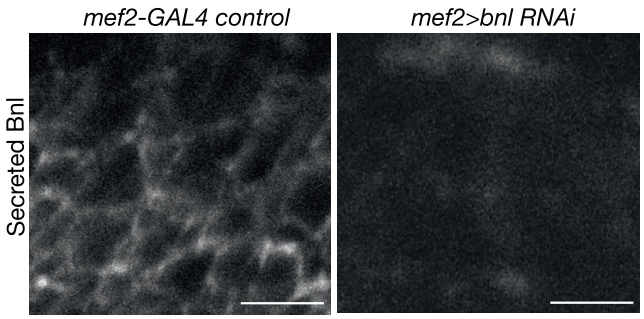

Figure S4. Effect of *bnl* RNAi on Secreted Bnl FGF Levels, Related to Figure 4

Interior views of indirect flight muscle fibers from control (;*mef-Gal4; UAS-CD8::GFP*) and muscle-specific *bnl* RNAi knockdown (;*mef2-Gal4*; *UAS-CD8::GFP/ UAS-bnl-RNAi*) pupa 55h APF that were immunostained for secreted Bnl (white) as in Figure 4. Animals also carried a *tubulin-Gal80ts* transgene and were raised at 18°C to inhibit expression of the RNAi transgenes during embryonic and larval development, then shifted to 30°C at 0h APF to allow Gal4-mediated induction of the *bnl* RNAi transgene during pupal life. Animals were fixed, stained, and imaged in parallel using identical settings. Note reduced extracellular Bnl in *bnl* RNAi knockdown, confirming specificity of immunostaining. Similar results were obtained in 4 independent experiments. Scale bar, 2 μm.

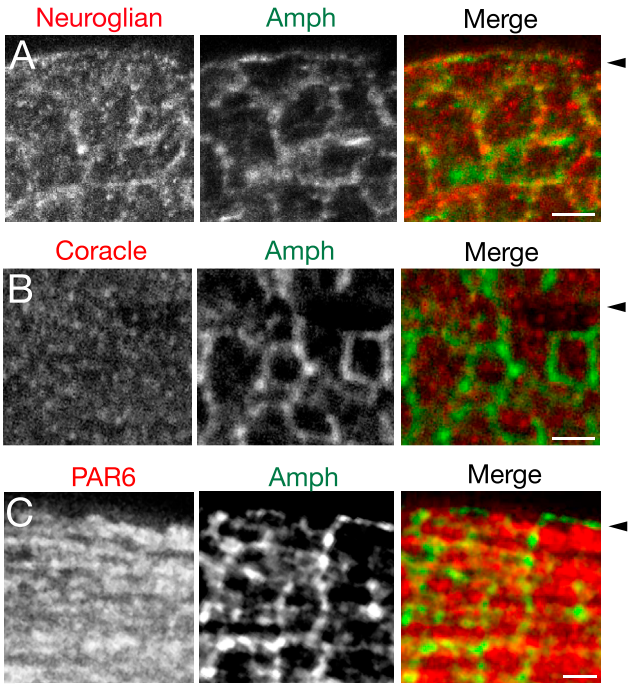

Figure S5. Expression and Localization of Epithelial Septate Junction and Polarity Module Proteins in Flight Muscle, Related to Figure 5

Interior views of indirect flight muscle fibers of a *mef2-Gal4*; *UAS-CD8-GFP* 55h APF pupa as in Figure 5 immunostained for the indicated proteins. Arrowhead, position of plasma membrane.

(A) Septate junction protein Neuroglian localizes preferentially to T-tubules.

(B) Coracle, part of the Yurt/Coracle basolateral identity module, is not detected above background level seen in other tissues.

(C) PAR6, part of the PAR apical identity complex, is detected but does not localize to specific membrane domain. Scale bars, 2 μm.

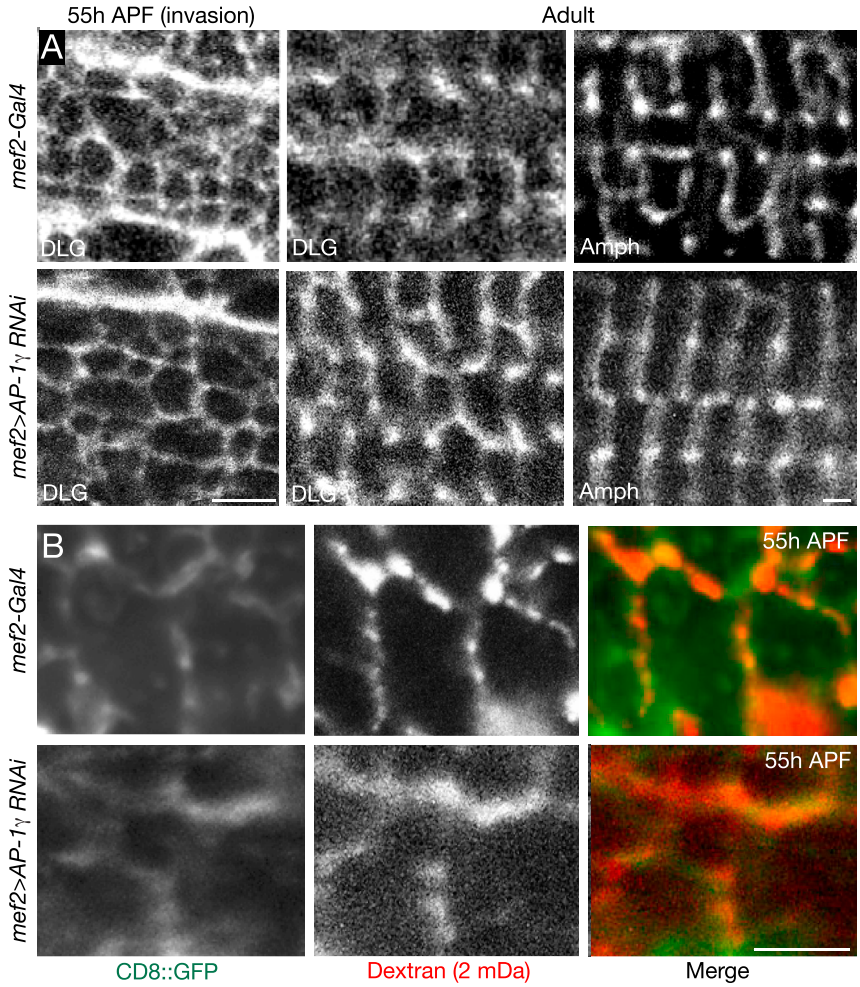

Figure S6. Effect of AP-1γ Knockdown on Flight Muscle T-Tubules, Related to Figure 6

(A) Interior view of indirect flight muscle fibers of control (;*mef-Gal4; UAS-CD8::GFP*; top panels) and muscle-specific AP-1γ knockdown (;*mef2-Gal4*; *UAS-CD8::GFP/UAS-AP-1γ RNAi*; bottom panels) pupa 55h APF (during tracheal invasion; left panels) and adult *Drosophila* (middle and right panels) immunostained for T-tubule markers Discs large (DLG, white) or amphiphysin (Amph, white) as indicated. There is little or no effect of AP-1γ knockdown on T-tubule biogenesis or T-tubule marker localization.

(B) Interior view of indirect flight muscle fibers of control and muscle-specific AP-1γ knockdown pupa at 55h APF as in A except that dissected muscles were incubated with fluorescent 2 mDa dextran beads (red) for 20 min and T-tubules visualized by endogenous CD8::GFP fluorescence (green). Note dextran in both control and AP-1γ knockdown muscle fibers, implying that the large surface openings to T-tubules are intact in AP-1γ knockdown. Scale bars, 2 μm.